Chemical Engineering Journal 144 (2008) 119–123

Contents lists available at ScienceDirect

Chemical Engineering Journal

journal homepage: www.elsevier.com/locate/cej

Various TiO_2 microcrystals: Controlled synthesis and enhanced photocatalytic activities

Fengyu Wei[a,b,*], Hualing Zeng[a], Peng Cui[a,b], Shuchuan Peng[c], Tianhu Cheng[c]

[a] *School of Chemical Engineering, Hefei University of Technology, Hefei 230009, China*
[b] *Anhui Key Laboratory of Controllable Chemical Reaction & Material Chemical Engineering, Hefei 230009, China*
[c] *School of Natural Resource and Environmental Engineering, Hefei University of Technology, Hefei 230009, China*

ARTICLE INFO

Article history:
Received 28 March 2008
Received in revised form 7 June 2008
Accepted 20 June 2008

Keywords:
Photocatalytic activity
TiO_2
Microspheres
Sedimentation

ABSTRACT

Titania microspheres with higher photocatalytic activity have been synthesized using $TiCl_4$ and $FeCl_3$ as the precursor in the presence of Span-80. The products were characterized with XRD, TEM and UV–vis DRS. XRD and TEM indicated that the microsphere was a mixture of rutile, brookite and anatase with a diameter of about 5–7 μm. The photocatalytic experiments revealed that the microspheres exhibited high photocatalytic activities under UV-light and solar irradiation. The degradation rate of methyl orange (MO) was 100% under UV-light irradiation for 3 h and 91% under solar irradiation for 6 h. In particular, the catalysts could be readily separated by sedimentation after the photocatalytic reaction.

© 2008 Elsevier B.V. All rights reserved.

1. Introduction

Titanium dioxide is one of the most popular and promising materials as a photocatalyst because it is stable in various solvents under photoirradiation, commercially available, and easy to be prepared in the laboratory [1,2]. However, its practical application seems to be limited for two reasons. One is the demand of the UV light as an essential excitating source due to its large band gap of 3.2 eV, and the other is that it is very difficult to separate these fine photocatalysts from solution after reaction. To enhance its photoactivity into visible range, considerable efforts have been taken including doping with various transition metal cations [3,4] and anions, such as Cr [5], Fe [6,7], V [8], N [9], S [10], etc. Although these doped TiO_2 photocatalysts could extend their optical sensibility to the visible range, the separation from solution after photocatalytic reaction is still a problem. In order to solve this problem, a general method is employed to immobilize the TiO_2 nanoparticles on a large substrate [11]. Although immobilization can improve the separation efficiently, it usually decreases the overall photocatalytic activity comparing to the dispersed TiO_2 due to lowering of the surface-to-volume ratio and partial loss of the active surface sites of photocatalysts. Therefore, it is necessary to develop a novel synthesis approach to prepare TiO_2 photocatalysts, which not only have highly photocatalytic activity, but also can be steadily separated after photocatalytic reactions. Recent years, the regular 3D structures, such as microspheres composed of uniform nanorods, have been exploited and anticipated as catalysts, electrical sensors and biologics [12,13]. Especially, these microspheres with large sizes could be readily separated from the solution by filtration or sedimentation, compared with the nanosized particles. Herein, we reported the fabrication of mixed-phase TiO_2 microspheres with Fe as a dopant, which performs highly photocatalytic activity and could be easily separated after photocatalytic reaction.

2. Experimental

2.1. Preparation of the TiO_2 photocatalysts

In a typical synthetic procedure, 5 ml of $TiCl_4$ solution mixed with 25 ml of 0.3 M $FeCl_3$ aqueous solution in the presence of 2 ml Span-80 with vigorous stirring. The transparent solution was transferred into a 50 ml Teflon-lined autoclave and sealed. The hydrothermal reaction was maintained at 180 °C for 48 h. The precipitate was separated by centrifugation and sequentially washed for several times by anhydrous alcohol and water until the pH was 7, and then dried at 60 °C overnight. The product was further calcinated at 400 °C for 2 h to remove surfactant and a few organic impurities. The as-prepared sample was donated as TiO_2–Fe–Span. Similarly, the sample obtained without using sur-

---

* Corresponding author at: School of Chemical Engineering, Hefei University of Technology, Tunxi Road 193, Hefei 230009, China. Tel.: +86 551 2901093; fax: +86 551 2901450.
E-mail address: weifyliuj@yahoo.com.cn (F. Wei).

1385-8947/$ – see front matter © 2008 Elsevier B.V. All rights reserved.
doi:10.1016/j.cej.2008.06.015

factant was donated as TiO_2–Fe, and the pure TiO_2 was prepared only using 25 ml of distilled H_2O with 5 ml of $TiCl_4$ solution.

2.2. Characterization

The XRD patterns were recorded on a Rigaku D/max-rB X-ray diffractometer using Cu Kα radiation ($\lambda = 1.5406$). Transmission electron microscopy (TEM) analysis was identified on a Hitachi H-800 with an accelerating voltage of 200 kV. The absorption edge and band gap energy of the samples were measured using a Shimadzu UV-240 spectrophotometer equipped with a diffuse reflectance accessory. The binding energy (BE) was identified by X-ray photoelectron spectroscopy (XPS) using a VGESCALAB-MK photoelectron spectrometer with an Mg Kα source.

2.3. Photocatalytic experiment

The photocatalytic activities of the prepared samples were evaluated by measuring the decomposition of 10 mg/l methyl orange (MO) aqueous solution. The UV-photocatalytic reactions were carried out in a glass immersion photochemical reactor charged with 900 ml MO aqueous solution, the concentration of catalyst was 0.1 g. An airflow was employed to produce a homogenous suspension of the catalyst in the solution, an 18 W low-pressure mercury lamp as UV-light source (wavelength 254 nm). The sunlight photocatalytic experiments were carried out in a vessel with the diameter of 15 cm. Because the intensity of sunlight is generally beyond our control, the sunlight photocatalytic experiments were performed at same time to ensure the consistency of the results. 0.1 g of the prepared catalyst was immersed into 300 ml MO aqueous solution with vigorous magnetic stirring. The average sunlight intensity striking on the surface of the reaction solution was about 65 klux, measured by Digital Illuminance Meter (TES Electrical Electronic Corp., TES-1335, China). Because the intensity of sunlight is generally beyond our control, the sunlight photocatalytic experiments were carried out at same time to ensure the consistency of the results. Prior to photocatalytic experiment, the suspension was stirring vigorously for 30 min in the dark to achieve the absorption equilibrium. The residual concentration of MO was detected on a Shimadzu UV-2550 spectrophotometer at 500 nm.

The photocatalytic activity can be quantitatively evaluated by comparing the removal efficiency (η (%)) of reactant. η (%) was calculated according to the following equation:

$$\eta(\%) = \frac{(A_0 - A)}{A_0} \times 100$$

where A_0 and A represent the initial equilibrium concentration and reaction concentration of reactant, respectively.

3. Results and discussion

3.1. Morphology and phase structure of the samples

The morphologies of samples were investigated by TEM. Fig. 1(A) shows that the TiO_2 nanorods with diameters of 60 nm and lengths of 500–800 nm were obtained by hydrothermal reaction using $TiCl_4$ and distilled water as starting materials. It can be seen clearly that the nanorods have uniform diameters and lengths. When $FeCl_3$ solution was added in hydrothermal reaction, the urchin-like microspheres with diameters of 1–2 μm were obtained (Fig. 1(B)). From the SEM image of the urchin-like microspheres, a large number of "pyramids" having a rectangular base (inset (B)) are found on the surface of these microspheres. As shown in Fig. 2(c), the urchin-like microspheres would alter to smooth spheres with the diameter of 5–7 μm when adding surfactant into reaction. It is inferred that surfactant and Fe may be favorable of the self-assembly of the nanorods. Up to now, the role of surfactant in this process is still unknown and need to research further. Han et al. [14] synthesized the rutile titania microspheres composed of radially aligned nanorods by hydrothermal reaction with $TiCl_3$ and $FeCl_2$. Liu et al. [15] prepared 3D TiO_2 microspheres through the reaction of $TiCl_3$ with urea in an *n*-butanol and water mixture at 150 °C assisted by a surfactant (Span-80). Their experiments showed that, without Span-80, only nanorods were obtained.

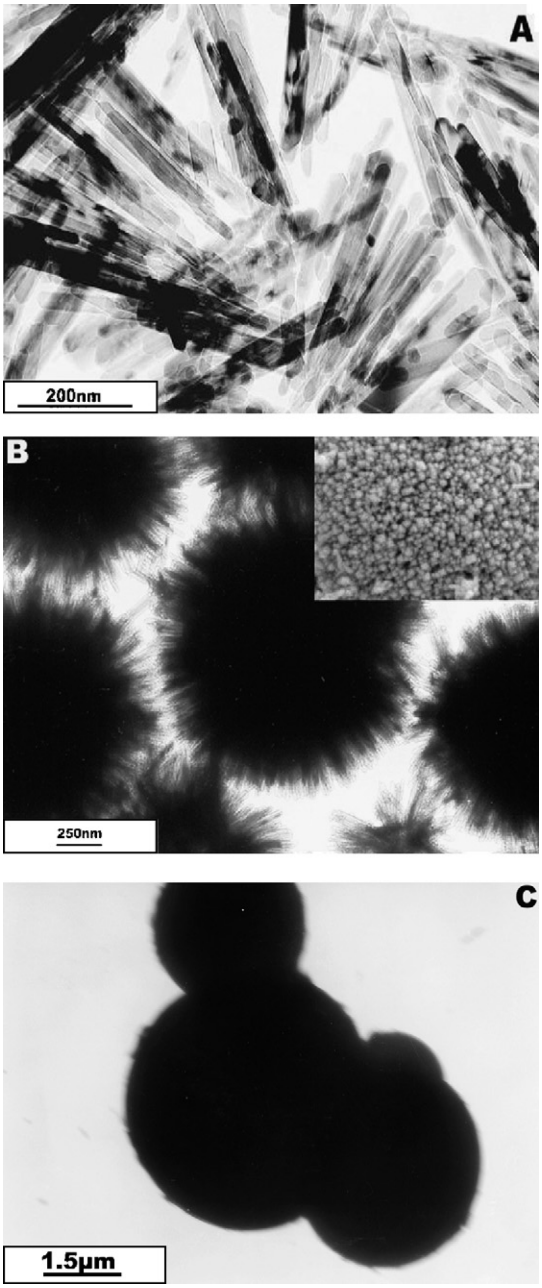

Fig. 1. TEM images of (A) TiO_2 and (B) TiO_2–Fe. Inset: corresponding SEM image of a microsphere's surface. (C) TiO_2–Fe–Span.

Fig. 2 shows the XRD patterns of the as-obtained samples. The diffraction peaks of the pure TiO_2 sample can be indexed to the rutile phase (JCPDS No. 21-1276). Fe-doped samples of TiO_2–Fe–Span and TiO_2–Fe are signed to have a major structure of rutile phase TiO_2 with a few of anatase and brookite phases. It would be inferred that the doping Fe could make the partial rutile convert

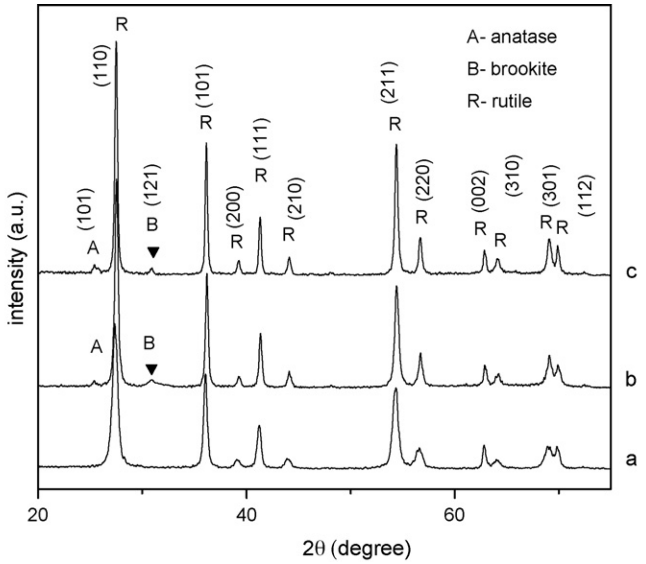

Fig. 2. XRD patterns of the TiO_2 photocatalysts (a) TiO_2 (b) TiO_2-Fe (c) TiO_2-Fe-Span.

to anatase TiO_2 which is very beneficial for photocatalytic degradation of organic contamination. To our surprise, no crystalline phase containing Fe could be observed in TiO_2–Fe and TiO_2–Fe–Span due to very low Fe concentration. Fe^{3+} and Ti^{4+} have similar ironic radii (0.79 Å vs. 0.75 Å), so Fe^{3+} can easily substitute Ti^{4+} into TiO_2 lattice [6,7,16].

3.2. XPS and UV–vis analysis

Determination of the oxidation state of the iron was carried out by measuring $Fe_{2p3/2}$ BE. Fig. 3 shows the high-resolution Fe2p XPS spectrum of the TiO_2–Fe–Span microspheres. Due to the BE of 710.7 eV assigned to Fe^{3+} [17], the oxidation state of iron in the lattices was probably Fe_2O_3. Possibly because of its low concentration and uniform distribution within TiO_2, iron phase could not be observed from XRD patterns in Fig. 2.

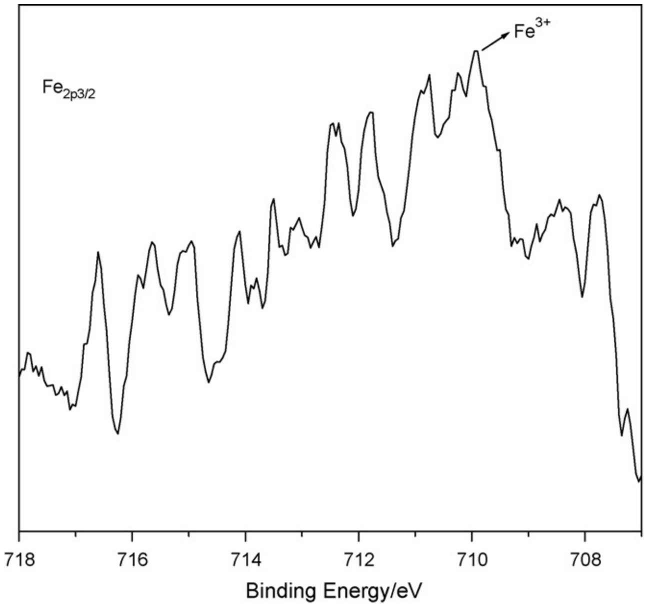

Fig. 3. High-resolution Fe2p XPS spectrum of TiO_2–Fe–Span.

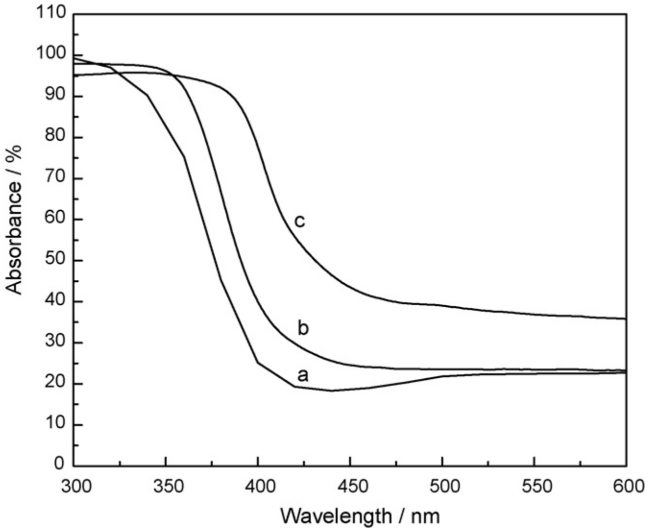

Fig. 4. UV–vis DRS of (a) TiO_2, (b) TiO_2–Fe and (c) TiO_2–Fe–Span.

Fig. 4 shows the UV–vis diffuse reflectance spectra of the TiO_2 samples. As shown in Fig. 4, the rutile TiO_2 nanorods exhibits an onset of the absorption at $\lambda_g = 406$ nm, while the TiO_2–Fe appears at about $\lambda_g = 430$ nm, and the TiO_2–Fe–Span at about $\lambda_g = 464$ nm. It is obvious that the absorption edge of TiO_2–Fe–Span had a remarkable shift to the visible light region. Lettmann et al. [18] had reported that increase of the light absorption in the visible region possibly result in better photocatalytic efficiency, especially under visible light irradiation. So it is a good way to obtain high vis-photocatalytic activity by improving its photoabsorption.

3.3. Photocatalytic activity

To evaluate the photocatalytic activities of catalysts, we studied the photodegradations of the MO over the above samples. However, the concentration of MO does not change using the as-prepared TiO_2 catalysts under the dark condition. Illumination in the absence of TiO_2 catalysts shows scarcely any photolytic activity. Therefore, the presence of both illumination and TiO_2 catalysts is necessary for the efficient degradation. Fig. 5 shows the photocatalytic activity of TiO_2–Fe–Span, TiO_2–Fe and TiO_2 under UV-light and sunlight irradiation. It is obvious that the TiO_2–Fe–Span possessed the highest photocatalytic activity. The decomposition rate of MO on TiO_2–Fe–Span was up to 100% under UV-light irradiation for 3 h and nearly to 91% for 6 h under solar irradiation. Rutile phase nanorods display a lower photocatalytic activity. Moreover, the decomposition rates of all samples under the UV-light illumination are higher than that under the sunlight illumination. Fig. 6 represents the UV–vis absorption spectra of MO on TiO_2–Fe–Span under UV-light and solar irradiation. The peak intensities of –N=N– chromophoric groups (500 nm) and benzenoid conjugate groups (310 nm) of MO molecules rapidly decreased with increasing of illumination time, indicating that MO was decomposed completely under UV-light illumination by TiO_2–Fe–Span.

Rutile is a thermodynamically stable phase and possesses a smaller band gap than that of anatase phase. According to the Hurum's explain [19], charges produced on rutile by visible light are stabilized through electron transfer to lower energy anatase lattice trapping sites. The transition points between the different phases allow for rapid electron transfer from rutile to anatase/brookite. Thus, rutile acts as an antenna to extend the photoactivity into visible wavelengths and the structural arrange-

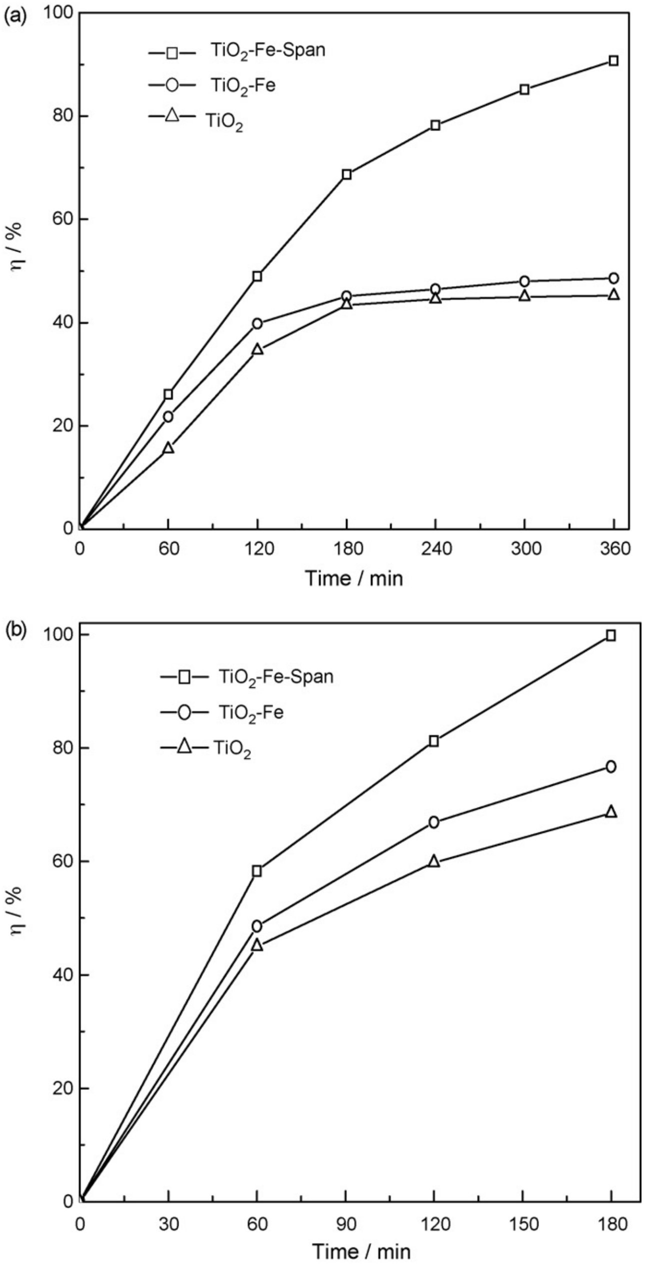

Fig. 5. Photocatalytic degradation of MO over photocatalysts under (a) solar and (b) UV-light irradiation.

ment of the TiO_2 crystallites creates catalytic “hot spots” at the rutile–anatase/brookite interfaces. Doping of Fe^{3+} has been affirmed to introduce much more oxygen vacancies in/on the crystal lattice and surface of TiO_2, while oxygen vacancies favor the adsorption of H_2O and the formation of surface hydroxyl group, which promote the photocatalytic activity [6]. The beneficial effect of Fe^{3+} could be further explained by considering the efficient separation of photo-excited electrons and holes [20]. Consequently, the higher photocatalytic activity of the microspheres is ascribed to a synergetic effect of the beneficial factors by Fe-doping and rutile, anatase and brookite mixing. For the TiO_2–Fe–Span, the surfactant Span-80 in the crystal voids would decompose and the surface area of the catalysts increased after calcined at high temperature. Therefore, it exhibited a higher photoactivity than the urchin-like microspheres obtained in the absence of Span-80.

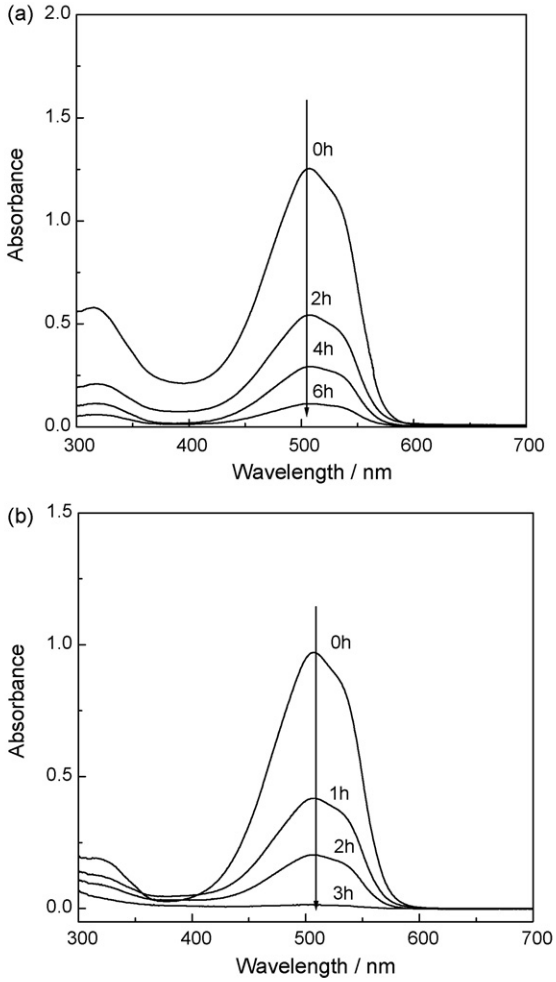

Fig. 6. UV–vis absorption spectra of MO in the presence of TiO_2–Fe–Span under (a) solar and (b) UV-light irradiation.

Furthermore, due to the large dimension of the microspheres, it can be easily separated from the reaction solution. Fig. 7 shows the sedimentation in aqueous suspensions of TiO_2–Fe–Span microspheres and TiO_2 nanoparticles. It is obvious that TiO_2–Fe–Span microspheres sedimentated from the aqueous suspension in less than 30 min (Fig. 7b–d), but TiO_2 nanoparticles were still turbid (Fig. 7a). TiO_2 microspheres catalysts with higher photocatalytic activity can be easily recovered by sedimentation, which will

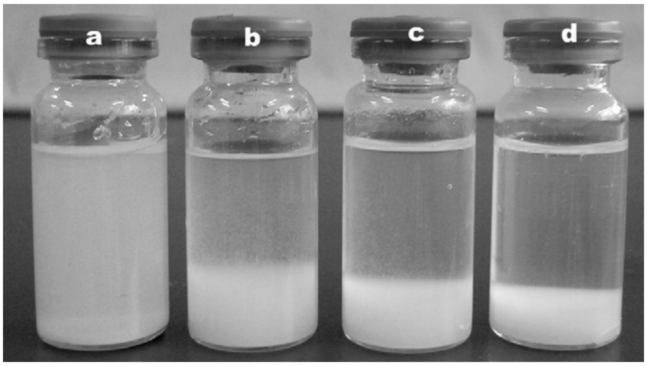

Fig. 7. Sedimentation in aqueous suspensions of (a) TiO_2 nanoparticles for 30 min and TiO_2–Fe–Span microspheres for (b) 5 min, (c) 15 min, and (d) 30 min.

greatly promote their industrial application to eliminate the organic pollutants in wastewater.

4. Conclusion

In summary, the mixed-phase TiO_2 microspheres were prepared by hydrothermal method at 180 °C for 48 h using $TiCl_4$ and $FeCl_3$ as precursor in the presence of surfactant Span-80. It exhibited excellent photocatalytic activities for photodegradation of MO both under solar and UV-light irradiations. It completely decomposed the MO and no intermediates were observed. Especially, the catalysts can be easily separated from solution by sedimentation after reaction. It is expected that the TiO_2 microspheres could be one of the ideal photocatalysts for the water purification.

Acknowledgements

This work was supported by the National Natural Science Foundation of China (No. 40672027) and Anhui Province Foundation of Natural Science Research (No. 070414166).

References

[1] M.R. Hoffmann, S.T. Martin, W.Y. Choi, D.W. Bahnemann, Environmental applications of semiconductor photocatalysis, Chem. Rev. 95 (1995) 69–96.
[2] A. Mills, S. Lehunte, An overview of semiconductor photocatalysis, J. Photochem. Photobiol. A 108 (1997) 1–20.
[3] W. Choi, A. Termin, M.R. Hoffmann, The role of metal ion in quantum-sized TiO_2 correlation between photoreactivity and charge carrier recombination dynamics, J. Phys. Chem. 98 (1990) 13669–13679.
[4] K.V.S. Rao, B. Lavédrine, P. Boule, Influence of metallic species on TiO_2 for the photocatalytic degradation of dyes and dye intermediates, J. Photochem. Photobiol. A 154 (2003) 189–193.
[5] M. Radecka, M. Wierzbicka, S. Komornicki, M. Rekas, Influence of Cr on photoelectrochemical properties of TiO_2 thin films, Phys. B 348 (2004) 160–168.
[6] J.F. Zhu, N.F. Chen, J.L. Zhang, H.J. Chen, M. Anpo, Fe^{3+}–TiO_2 photocatalysts prepared by combining sol–gel method with hydrothermal treatment and their characterization [J], J. Photochem. Photobiol. A: Chem. 180 (2006) 196–204.
[7] M.S. Nahar, K. Hasegawa, S. Kagaya, S. Kuroda, Comparative assessment of the efficiency of Fe-doped TiO_2 prepared by two doping methods and photocatalytic degradation of phenol in domestic water suspensions, Sci. Technol. Adv. Mater. 8 (2007) 286–291.
[8] J.C.S. Wu, C.H. Chen, A visible-light response vanadium-doped titania nanocatalyst by sol–gel method, J. Photochem. Photobiol. A: Chem. 163 (2004) 509–515.
[9] T. Ohno, M. Akiyoshi, T. Umebayashi, K. Asai, T. Mitsui, M. Matsumura, Preparation of S-doped TiO_2 photocatalysts and their photocatalytic activities under visible light, Appl. Catal. A 265 (2004) 115–121.
[10] R. Asahi, T. Morikawa, T. Ohwaki, K. Aoki, Y. Taga, Visible-light photocatalysis in nitrogen-doped titanium oxides, Science 293 (2001) 269–271.
[11] K.V.S. Rao, A. Rachel, M. Subrahnyam, P. Boule, Immobilization of TiO_2 on pumice stone for the photocatalytic degradation of dyes and dye industry pollutants, Appl. Catal. B: Environ. 46 (2003) 77–85.
[12] Y. Sheng, B. Zhou, Y.H. Liu, X. Zhao, C.Y. Wang, Y. Pan, Z.C. Wan, Close-packed nano-TiO_2 anatase microspheres synthesis and their luminescent properties, Mater. Lett. 60 (2006) 1327–1330.
[13] H.G. Yang, H.C. Zeng, Preparation of hollow anatase TiO_2 nanospheres via ostwald ripening, J. Phys. Chem. B 108 (2004) 3492–3495.
[14] Y. Han, G.C. Li, Z.K. Zhang, Synthesis and optical properties of rutile TiO_2 microspheres composed of radially aligned nanorods, J. Cryst. Growth 295 (2006) 50–53.
[15] L. Liu, Y.P. Zhao, H.J. Liu, H.Z. Kou, Y.Q. Wang, Directed growth of TiO_2 nanorods into microspheres, Nanotechnology 17 (2006) 5046–5050.
[16] J.F. Zhu, W. Zheng, B. Bin, J.L. Zhang, M. Anpo, Characterization of Fe–TiO_2 photocatalysts synthesized by hydrothermal method and their photocatalytic reactivity for photodegradation of XRG dye diluted in water, J. Mol. Catal. A: Chem. 216 (2004) 35–43.
[17] J.G. Yu, H.G. Yu, C.H. Ao, S.C. Lee, J.C. Yu, W.K. Ho, Preparation, characterization and photocatalytic activity of in situ Fe-doped TiO_2 thin films, Thin Solid Films 496 (2006) 273–280.
[18] C. Lettmann, K. Hildenbrand, H. Kisch, W. Macyk, W.F. Maier, Visible light photodegradation of 4-chlorophenol with a coke-containing titanium dioxide photocatalyst, Appl. Catal. B: Environ. 32 (2001) 215–227.
[19] D.C. Hurum, A.G. Agrios, K.A. Gray, Explaining the enhanced photocatalytic activity of Degussa P25 mixed-phase TiO_2 using EPR, J. Phys. Chem. B 107 (2003) 4545–4549.
[20] T. Ohno, Z. Miyamoto, K. Nishijima, H. Kanemitsu, X.Y. Feng, Sensitization of photocatalytic activity of S- or N-doped TiO_2 particles by adsorbing Fe^{3+} cations, Appl. Catal. A: Gen. 302 (2006) 62–68.